Iranian Journal of Science and Technology, Transactions of Civil Engineering (2020) 44:683–693
https://doi.org/10.1007/s40996-019-00271-1

RESEARCH PAPER

Modified Pseudo-dynamic Bearing Capacity of Shallow Strip Footing Considering Fully Log-Spiral Passive Zone with Global Center

Arijit Saha[1] · **Sima Ghosh**[1]

Received: 25 April 2016 / Accepted: 23 May 2019 / Published online: 3 June 2019

Abstract

The subject seismic bearing capacity is one of the most important aspects of geotechnical earthquake engineering. As the existing pseudo-dynamic method has certain drawbacks, this paper presents a modified pseudo-dynamic approach to evaluate the seismic bearing capacity of shallow strip footing resting on c–Φ soil considering the log-spiral failure mechanism. Since damping is present in all materials, more realistic results can be obtained by modeling the soil as a visco-elastic material. Here, the passive failure region is considered a fully log-spiral zone with an arbitrary location of the center of log-spiral. A single seismic bearing capacity coefficient ($N_{\gamma e}$) is evaluated for the simultaneous resistance of unit weight, surcharge and cohesion, which is more practical to simulate the field failure mechanism. The effects of soil and seismic parameters are taken into account to evaluate the seismic bearing capacity of the foundation. The results obtained from the present analysis are presented in both tabular and graphical non-dimensional form. Results are thoroughly compared with the existing values in the literature, and a reasonably good agreement is found with the existing studies.

Keywords Modified pseudo-dynamic bearing capacity · Log-spiral failure mechanism with global center · c–Φ soil · Single bearing capacity coefficient

List of symbols

$2c/\gamma B_0$	Cohesion factor
B_0	Width of the footing
Φ	Angle of internal friction of the soil
C	Unit cohesion of soil
D_f	Depth of footing below ground surface
D_f/B_0	Depth factor
R	Reaction force
G	Acceleration due to gravity
G	Shear modulus of soil
k_h, k_v	Horizontal and vertical seismic accelerations
m	Mobilization factor
$N_{\gamma e}$	Optimized single seismic bearing capacity coefficient
P_L	Uniformly distributed column load
P_p	Passive earth pressure resistance
Q	Surcharge loadings
r_0, r_f	Initial and final radii of the log-spiral zone (i.e., BE and BD), respectively
α_1, α_2	Base angles of the triangular elastic zone under the foundation
θ	Angle that makes the log-spiral part in log-spiral mechanism
γ	Unit weight of soil medium
γ_s	Shear strain
η	Soil viscosity
t	Time
ξ	Damping ratio
ρ	Mass density of the soil medium
τ	Shear stress
υ	Poisson's ratio of the soil medium
ω	Angular frequency
c_m	Mobilized unit cohesion
Φ_m	Mobilized angle of internal friction of the soil

1 Introduction

Structural foundations are the substructure elements which transmit the structural load to the earth in such a way that the supporting soil is not overstressed and does not undergo

✉ Arijit Saha
sahaarijit20@gmail.com

Sima Ghosh
simacvl@gmail.com

[1] NIT Agartala, Agartala, India

deformations that would cause excessive settlement of the structure. The evaluation of bearing capacity of shallow strip footing under seismic loading condition is an important phenomenon in the earthquake-prone region. The pioneering works in determining the bearing capacity in static condition were done by Prandtl (1921), Terzaghi (1943), Meyerhoff (1957), (1963), Vesic (1973), Saran and Agarwal (1991) and many others. Geotechnical Earthquake researchers have investigated the problem of seismic bearing capacity of foundation using different mechanisms. The design of foundation in seismic areas needs special consideration compared to the static case. A number of researchers had analyzed the seismic bearing capacity of shallow strip footings using the pseudo-static approach with the help of different solution techniques such as the method of slices, limit equilibrium, method of stress characteristics an upper bound limit analysis. Budhu and Al-karni (1993), Dormieux and Pecker (1995), Soubra (1993), (1997), (1999), Richards et al. 1993, Choudhury and Subha Rao (2005), Kumar and Ghosh (2006) and many more had considered the effect of earthquake on the bearing capacity of a surface to a shallow strip footing under pseudo-static method using different approaches. IS 6403 1981 also gives a formulation of ultimate bearing capacity for different types of shallow foundations in different types of soils considering pseudo-static method. In the pseudo-static method, the dynamic nature of earthquake loading is considered in a very approximate way without taking any effect of time, frequency and soil amplification. To overcome this drawback, Ghosh (2008), Ghosh and Choudhury (2011), Saha and Ghosh (2014) give solutions of pseudo-dynamic bearing capacity of shallow strip footing considering the Coulomb failure mechanism using limit analysis method and limit equilibrium method, respectively. Later on, Saha and Ghosh (2015) analyzed pseudo-dynamic bearing capacity using composite failure mechanism.

But the current form of the pseudo-dynamic method does not satisfy the zero stress boundary condition at the ground surface, and it requires assuming an amplification factor as the acceleration value amplifies linearly toward the ground surface and does not consider energy dissipation as all materials have some damping properties. Considering visco-elastic behavior of soil material, Bellezza (2014) and Bellezza (2015) proposed a modified pseudo-dynamic method to analyze soil-retaining wall which overcomes all those mentioned limitations. Later on, Pain et al. (2015a, b) and Pain et al. (2016) carried out this modified pseudo-dynamic method to analyze the seismic stability of retaining wall, the uplift capacity of horizontal strip anchors and bearing capacity of strip footings, respectively. In this paper, an attempt is made to solve this problem of bearing capacity of shallow strip footing considering log-spiral failure mechanism using modified pseudo-dynamic approach. Here in this analysis, the active region is considered linear with the logarithmic passive region. Unlike the earlier assumption, the passive failure region is considered as fully log-spiral zone despite composite failure surface. In this passive region, the center of the log-spiral curve is arbitrarily chosen and the bearing capacity coefficient optimized for not only different radii angle subtended by those radii at the center but also for different locations of the center of the log-spiral curve. To evaluate the bearing capacity under seismic loading condition, the simultaneous resistance of unit weight, surcharge and cohesion are taken into account, and a single seismic bearing capacity coefficient ($N_{\gamma e}$) is presented here. Results are presented in both tabular and graphical non-dimensional form including comparison with other available methods. Effects of wide range of variation of parameters such as soil friction angle (Φ), cohesion factor ($2c/\gamma B_0$), depth factor (D_f/B_0), mobilization factors (m) and horizontal and vertical seismic accelerations (k_h, k_v) along with primary wave and shear wave velocity on the pseudo-dynamic bearing capacity coefficient ($N_{\gamma e}$) have been studied.

2 Method of Analysis

In this paper, an attempt has been made to give a formulation of modified pseudo-dynamic bearing capacity of a shallow strip footing resting on c–Φ soil using limit equilibrium method. The homogeneous soil of effective unit weight γ has Mohr–Coulomb characteristic c–Φ soil and can be considered as a rigid plastic body. Let us consider a shallow strip footing of width (B_0) resting below the ground surface at a depth of (D_f) over which a column load (P) acts vertically with the overburden pressure over the level BD acting as a surcharge ($q = \gamma D_f$). The extension of the failure surface is shown in Fig. 1. ΔABE is the active zone just below the foundation. BDE is the log-spiral passive zone with the arbitrarily chosen center of the log-spiral curve at one side of the center line of the foundation. The soil on the other side of the center line gets partially mobilized, and this is characterized by a mobilization factor m. The shear strength of the soil is expressed as $\tau = mc + \sigma \tan \phi_m$, where $\phi_m = \tan^{-1}(m \tan \phi)$. It is a log-spiral failure mechanism that is defined by the angular parameters α_1, α_2, θ and β.

The radial log-spiral shearing zone BED is bounded by a log-spiral curve ED, where the equation for the curve in polar coordinates (r, θ_x) is $r = r_0 e^{\theta_x \tan \phi}$. The center of this log-spiral ED is at an arbitrary point O, and the initial radius r_0 is the length of the line OE.

where $\overline{OE} = r_0 = \frac{B_0 \sin \alpha_1 \sin \alpha_2}{\sin(\alpha_1+\alpha_2)\{\sin(\theta+\beta) - e^{\theta \tan \phi} \sin \beta\}}$

$\alpha_2 = \tan^{-1}(m \tan \alpha_1)$ and the final radius r_f (OD) is given by $r_f = r_0 e^{\theta \tan \phi}$.

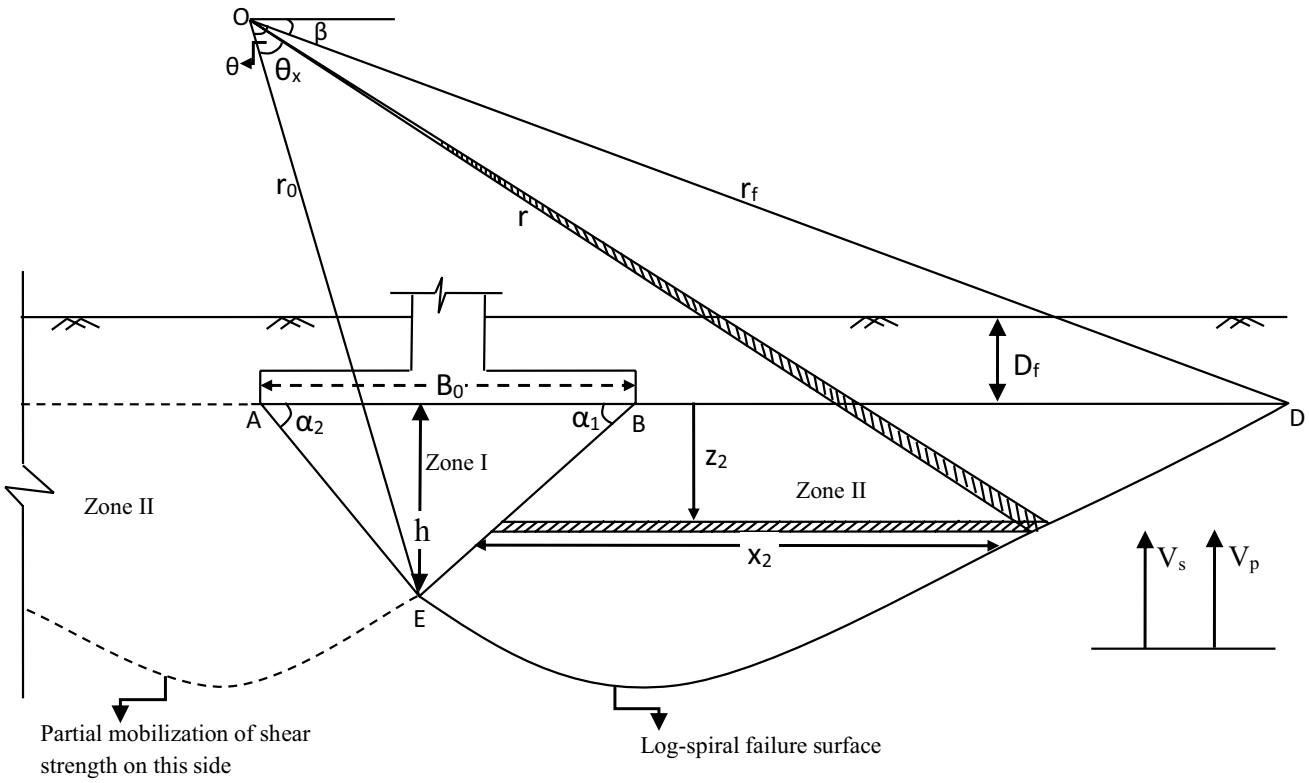

Fig. 1 Log-spiral failure mechanism

Figure 2a and b shows the detailed free-body diagram of elastic zone ABE and log-spiral shear zone BED, respectively.

2.1 Wave Propagation Through Visco-Elastic Soil Media

In real materials, the elastic energy of a traveling wave is always converted to heat for which the amplitude of the wave decreases. In visco-elastic wave propagation, soils are usually modeled as Kelvin–Voigt solids. A purely elastic spring and a purely viscous dashpot are connected in parallel in this type of model. The resistance to shearing deformation is the sum of an elastic component and a viscous component in 2D Kelvin–Voigt model (Kramer 1996).

$$\tau = 2\gamma_s G + 2\eta\frac{\partial\gamma_s}{\partial t} \tag{1}$$

where τ is the shear stress, γ_s is shear strain, η is the soil viscosity, G is the shear modulus and t is the time.

The equation of motion of Kelvin–Voigt visco-elastic medium in vectorial form (Yuan et al. 2006) is given by

$$\rho\frac{\partial^2 U}{\partial t^2} = \left\{(\lambda+G)+\left(\eta_1+\eta_s\right)\frac{\partial}{\partial t}\right\}\mathrm{grad}(\theta)+\left(G+\eta_s\frac{\partial}{\partial t}\right)\nabla^2 U \tag{2}$$

where ρ is the soil density, U is the displacement vector of components u_x, u_y and u_z and $\theta = \mathrm{div}(U)$.

Considering wave propagating along the z-axis in a Kelvin–Voigt homogeneous medium, a solution of Eq. (2) yields

$$\rho\frac{\partial^2 u_h}{\partial t^2} = G\frac{\partial^2 u_h}{\partial z^2}+\eta_s\frac{\partial^3 u_h}{\partial t\partial z^2} \tag{3}$$

$$\rho\frac{\partial^2 u_v}{\partial t^2} = (\lambda+2G)\frac{\partial^2 u_v}{\partial z^2}+\left(\eta_1+2\eta_s\right)\frac{\partial^3 u_v}{\partial t\partial z^2} \tag{4}$$

where $u_h = u_x$ and $u_v = u_z$.

For harmonic waves, solution of the equation of motion may be written as

$$u(z,t) = Ae^{i(\omega t-k^* z)}+Be^{i(\omega t+k^* z)} \tag{5}$$

where A and B are the constants that depend on boundary condition and k^* is the complex wave number, i.e., $k^* = \omega\sqrt{\frac{\rho}{G^*}}$

G^* = the complex shear modulus = $G(1+2i\xi)$

According to Kolsky (1963), k^* is given by $k^* = k_1 + ik_2$.

2.1.1 Expression of Horizontal Acceleration

For harmonic shaking, $\eta_s = \frac{2G\xi_s}{\omega_s}$, where ξ_s = damping ratio. Applying the boundary condition, i.e., shear stress at the free

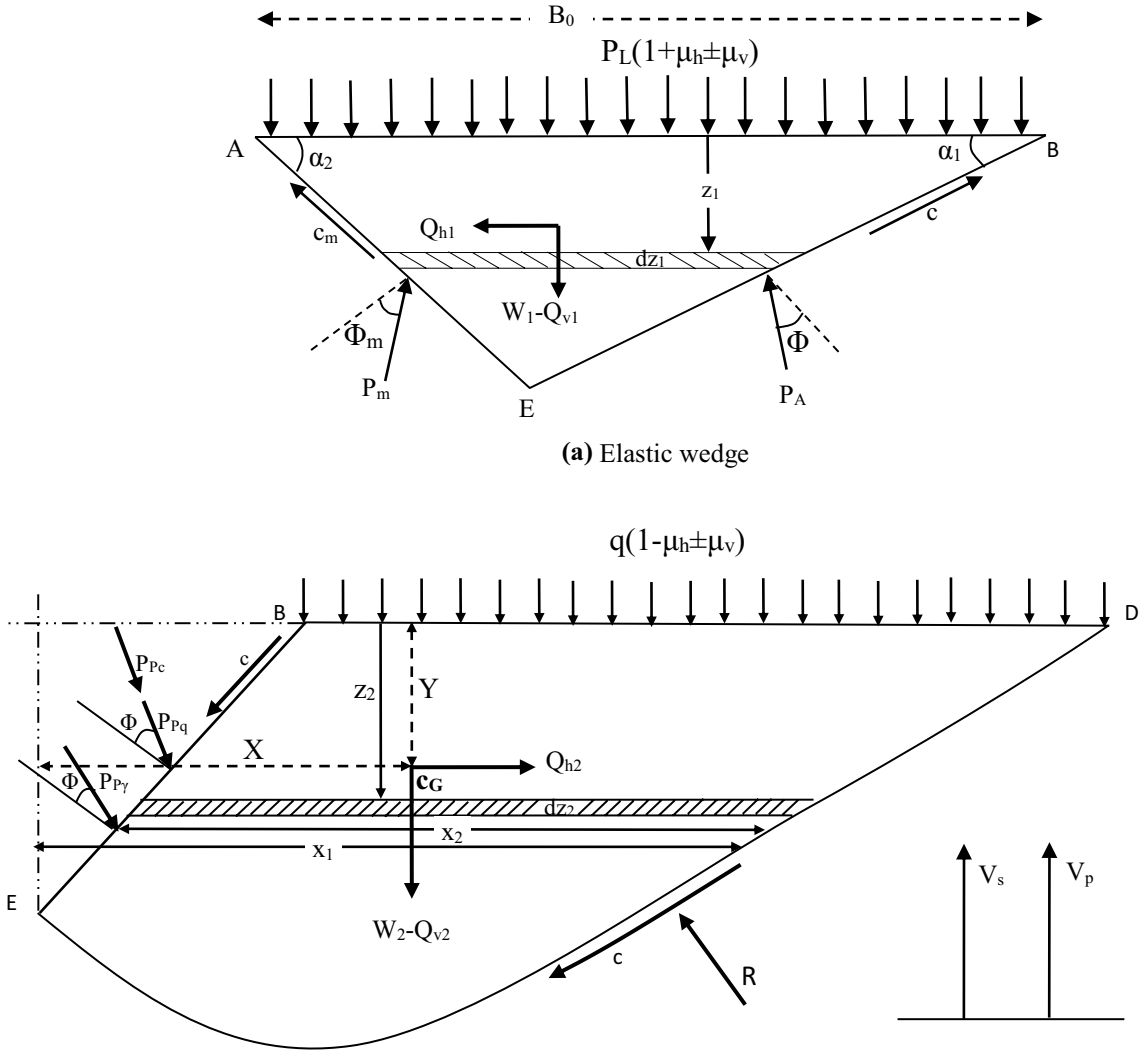

(a) Elastic wedge

(b) Log-spiral zone

Fig. 2 **a** Elastic wedge. **b** Log-spiral zone

surface $z=0$ and at a depth $z=H$ the displacement coincides with the rigid base, $u_b = u_{h0}e^{i\omega t}$ solution of Eq. (5) yields

$$A = B = \frac{u_{h0}}{2\cos(k^*H)}$$

So,

$$u(z,t) = u_{ho}e^{i\omega t}\frac{\cos(k^*z)}{\cos(k^*H)} \tag{6}$$

Differentiating Eq. (5) twice w.r.t. time and defining $k_h g = -\omega_s^2 u_{h0}$, the real part of horizontal acceleration is expressed as (Bellezza 2014)

$$a_h(z,t) = \frac{k_h g}{c_s^2 + s_s^2}\left[\left(c_s c_{sz} + s_s s_{sz}\right)\cos(\omega_s t) + \left(s_s c_{sz} - c_s s_{sz}\right)\sin(\omega_s t)\right] \tag{7}$$

2.1.2 Expression of Vertical Acceleration

For vertical harmonic motion, Eq. (4) can be written in a form similar to Eq. (3) provided that u_h, G and η_s are replaced by u_v, $E_c = (\lambda + 2G)$ and $\eta_p = \left(\eta_1 + 2\eta_s\right)$, respectively. Similarly, applying the boundary condition, i.e., shear stress at the free surface $z=0$ and at a depth, $z = h$ the displacement coincides with the rigid base, $u_b = u_{v0}e^{i\omega t}$ Then, the real part of vertical acceleration defining $k_v g = -\omega_p^2 u_{v0}$ can be obtained as (Bellezza 2015)

$$a_v(z,t) = \frac{k_v g}{c_p^2 + s_p^2}\left[\left(c_p c_{pz} + s_p s_{pz}\right)\cos(\omega_p t) + \left(s_p c_{pz} - c_p s_{pz}\right)\sin(\omega_p t)\right] \tag{8}$$

2.2 Bearing Capacity Expression

2.2.1 Elastic Wedge

The forces acting on the wedge include uniformly distributed total column load P on AB; horizontal and vertical inertia forces (Q_{h1} and Q_{v1}) are acting at the center of ΔABE. Active earth pressure P_A and cohesion c are acting on the side BE, whereas mobilized cohesion $c_m\left(c_m = mc\right)$ and mobilized active earth pressure P_m are acting on the face of AE, respectively.

The mass of a thin element of the elastic wedge at depth z_1 (Fig. 2a) is

$$m(z_1) = \frac{\gamma}{g}\left(\cot\alpha_1 + \cot\alpha_2\right)\left(h - z_1\right)\mathrm{d}z_1 \tag{9}$$

where$h = \frac{B_0 \sin\alpha_1 \sin\alpha_2}{\sin\left(\alpha_1+\alpha_2\right)}$and weight of the wedge ABE,

$$W_1 = \int_0^h m(z_1)\cdot g = \frac{\gamma}{2}B_0^2\frac{\sin\alpha_1\sin\alpha_2}{\sin\left(\alpha_1+\alpha_2\right)} \tag{10}$$

If the base of the foundation is subjected to a harmonic horizontal seismic acceleration of amplitude $k_h g$ at any depth z_1 and time t, below the base of the foundation, the total horizontal inertia force acting within the elastic zone (Fig. 2a) can be expressed as follows:

$$\begin{aligned} Q_{h1} &= \int_0^h m(z_1)a_h(z_1,t)\mathrm{d}z_1 \\ &= \frac{\gamma k_h h^2\left(\cot\alpha_1+\cot\alpha_2\right)}{\left(c_s^2+s_s^2\right)\left(y_{s1}^2+y_{s2}^2\right)^2} \\ &\left[\begin{array}{l}\left(c_s\cos\omega t + s_s\sin\omega t\right)\left\{2y_{s1}y_{s2}\sin y_{s1}\sinh y_{s2} - \left(y_{s1}^2-y_{s2}^2\right)\left(\cos y_{s1}\cosh y_{s2}-1\right)\right\} \\ +\left(s_s\cos\omega t - c_s\sin\omega t\right)\left\{2y_{s1}y_{s2}\left(\cos y_{s1}\cosh y_{s2}-1\right) + \left(y_{s1}^2-y_{s2}^2\right)\sin y_{s1}\sinh y_{s2}\right\}\end{array}\right] \end{aligned} \tag{11}$$

Similarly, as horizontal inertia force, the vertical inertia force acting within the elastic zone (Fig. 2a) can be expressed as follows:

$$\begin{aligned} Q_{v1} &= \int_0^h m(z_1)a_v(z_1,t)\mathrm{d}z_1 \\ &= \frac{\gamma k_v h^2\left(\cot\alpha_1+\cot\alpha_2\right)}{\left(c_p^2+s_p^2\right)\left(y_{s1}^2+y_{s2}^2\right)^2} \\ &\left[\begin{array}{l}\left(c_p\cos\omega t + s_p\sin\omega t\right)\left\{2y_{p1}y_{p2}\sin y_{p1}\sinh y_{p2} - \left(y_{p1}^2-y_{p2}^2\right)\left(\cos y_{p1}\cosh y_{p2}-1\right)\right\} \\ +\left(s_p\cos\omega t - c_p\sin\omega t\right)\left\{2y_{p1}y_{p2}\left(\cos y_{p1}\cosh y_{p2}-1\right) + \left(y_{p1}^2-y_{p2}^2\right)\sin y_{p1}\sinh y_{p2}\right\}\end{array}\right] \end{aligned} \tag{12}$$

where

$c_s = \cos\left(y_{s1}\right)\cosh\left(y_{s2}\right);\ s_s = -\sin\left(y_{s1}\right)\sinh\left(y_{s2}\right)$

$c_p = \cos\left(y_{p1}\right)\cosh\left(y_{p2}\right);\ s_p = -\sin\left(y_{p1}\right)\sinh\left(y_{p2}\right)$

$$y_{s1} = k_1 h = \frac{\omega_s h}{V_s}\left(\frac{\left(1+4\xi_s^2\right)^{1/2}+1}{2\left(1+4\xi_s^2\right)}\right)^{1/2};$$

$$y_{s2} = k_2 h = -\frac{\omega_s h}{V_s}\left(\frac{\left(1+4\xi_s^2\right)^{1/2}-1}{2\left(1+4\xi_s^2\right)}\right)^{1/2}$$

and $y_{p1} = \frac{\omega_p h}{V_p}\left(\frac{\left(1+4\xi_p^2\right)^{1/2}+1}{2\left(1+4\xi_p^2\right)}\right)^{1/2};\ y_{p2} = -\frac{\omega_p h}{V_p}\left(\frac{\left(1+4\xi_p^2\right)^{1/2}-1}{2\left(1+4\xi_p^2\right)}\right)^{1/2}$

Considering the force equilibrium conditions ($\sum V = \sum H = 0$) on the elastic wedge ABE

$$\begin{aligned} P_L B_0\left(1\pm\mu_v\right) = {} & P_A\cos\left(\alpha_1-\phi\right) + P_m\cos\left(\alpha_2-\phi_m\right) \\ & - W_1 \pm Q_{v1} + \frac{cB_0\sin\alpha_1\sin\alpha_2}{\sin\left(\alpha_1+\alpha_2\right)} \\ & + \frac{c_m B_0\sin\alpha_2\sin\alpha_1}{\sin\left(\alpha_1+\alpha_2\right)} \end{aligned} \tag{13}$$

$$P_{\mathrm{L}}B_0\mu_{\mathrm{h}} = P_{\mathrm{A}}\sin\left(\alpha_1-\phi\right) - P_m\sin\left(\alpha_2-\phi_m\right) - Q_{\mathrm{h1}} - \frac{cB_0\cos\alpha_1\sin\alpha_2}{\sin\left(\alpha_1+\alpha_2\right)} + \frac{c_mB_0\cos\alpha_2\sin\alpha_1}{\sin\left(\alpha_1+\alpha_2\right)} \quad (14)$$

So,

$$P_{\mathrm{L}} = \frac{\left[\begin{array}{l} P_{\mathrm{A}}\left\{\sin\left(\alpha_1-\phi\right)+\cos\left(\alpha_1-\phi\right)\right\} - P_m\left\{\sin\left(\alpha_2-\phi_m\right)-\cos\left(\alpha_2-\phi_m\right)\right\} - W_1 \pm Q_{\mathrm{v1}} \\ -Q_{\mathrm{h1}} + \dfrac{cB_0}{\sin\left(\alpha_1+\alpha_2\right)}\left\{\sin\alpha_2\left(\sin\alpha_1-\cos\alpha_1\right)+m\sin\alpha_1\left(\sin\alpha_2+\cos\alpha_2\right)\right\} \end{array}\right]}{B_0\left\{1+\mu_{\mathrm{h}}\pm\mu_{\mathrm{v}}\right\}} \quad (15)$$

where $\mu_{\mathrm{h}} = k_{\mathrm{h}}\sin 2\pi\left(\frac{t}{T}-0.3\right)$ and $\mu_{\mathrm{V}} = k_{\mathrm{V}}\sin 2\pi\left(\frac{t}{T}-0.16\right)$

Equilibrium P_{A} as obtained from active zone must be equal to passive earth pressure P_{p} of the passive zone. So,

$$P_{\mathrm{A}} = P_{\mathrm{P}} \quad (16)$$

where $P_P = P_{P\gamma} + P_{Pq} + P_{Pc}$ and $P_m = P_{m\gamma} + P_{mq} + P_{mc}$

Passive earth resistances $P_{\mathrm{p}\gamma}$, $P_{\mathrm{p}q}$ and $P_{\mathrm{p}c}$ are determined by considering the moment equilibrium of the forces which are acting on the soil mass BED (log-spiral passive zone) as shown in Fig. 2b.

2.2.2 Log-Spiral Shear Zone

Let us consider a thin elemental horizontal strip of thickness $\mathrm{d}z_2$ at any depth z_2 from the footing surface. At an angle θ_x, the radius (r) of the logarithmic spiral may be expressed as $r = r_0e^{\theta_x\tan\phi}$; the length of this strip from the same depth z_2 is assumed as x_2. So, the mass of strip of the log-spiral zone BDE (Fig. 2b):

$$m(z_2) = \frac{\gamma}{g}x_2\mathrm{d}z_2 \quad (17)$$

where $x_2 = r_0\left[e^{\theta_x\tan\phi}\left\{\cos\left(\beta+\theta-\theta_x\right)-\cot\alpha_1\sin\left(\beta+\theta-\theta_{\mathrm{x}}\right)\right\} - \cos\left(\beta+\theta\right)+e^{\theta\tan\phi}\sin\left(\theta+\beta\right)\cot\alpha_1\right]$

$\mathrm{d}z_2 = r_0e^{\theta_x\tan\phi}\left[\tan\phi\sin\left(\beta+\theta-\theta_x\right)-\cos\left(\beta+\theta-\theta_x\right)\right]\mathrm{d}\theta_x$

So, weight of the log-spiral shear zone BDE,

$$W_2 = g\int_0^{\theta} m\left(z_2\right)\cdot\mathrm{d}z_2 = I_1 \quad (18)$$

The horizontal and vertical inertia forces acting on the log-spiral shear zone can be expressed as follows:

$$Q_{\mathrm{h2}} = \int_0^{\theta} m\left(z_2\right)a_{\mathrm{h}}(z,t)\mathrm{d}z_2 = I_2 \quad (19)$$

$$Q_{\mathrm{v2}} = \int_0^{\theta} m\left(z_2\right)a_{\mathrm{v}}(z,t)\mathrm{d}z_2 = I_3 \quad (20)$$

The intensity of surcharge $q = \gamma D_{\mathrm{f}}$, where γ is the unit weight of soil and D_{f} is the depth of footing, acts as uniformly distributed over BH. So, the force due to surcharge load q

$$Q = \gamma D_{\mathrm{f}}\cdot\overline{\mathrm{BD}}\left(1-\mu_{\mathrm{h}}\pm\mu_{\mathrm{v}}\right) \quad (21)$$

where $\overline{\mathrm{BD}} = r_0e^{\theta\tan\phi}\cos\beta - r_0\cos\left(\theta+\beta\right) - \frac{B_0\sin\alpha_2\cos\alpha_1}{\sin\left(\alpha_1+\alpha_2\right)}$.

Taking moment equilibrium of the forces acting on the log-spiral failure zone BED about the center of the log-spiral (O), we get

$$P_{\mathrm{P}\gamma}\left[\overline{OY}\right] = \left(W_2\pm Q_{\mathrm{v2}}\right)\left[X+r_0\cos\left(\beta+\theta\right)\right] - Q_{\mathrm{h2}}\left[Y+r_{\mathrm{f}}\sin\beta\right] \quad (22)$$

$$\left(P_{\mathrm{P}q}-P_{\mathrm{P}c}\right)\left[\overline{OX}\right] = Q\left[0.5\overline{\mathrm{BD}} + \frac{B_0\cos\alpha_1\sin\alpha_2}{\sin\left(\alpha_1+\alpha_2\right)} + r_0\cos\left(\beta+\theta\right)\right] + cr_0^2\left[\frac{\left(e^{2\theta\tan\phi}-1\right)}{2\tan\phi} + \frac{\sin\left(\theta+\beta+\alpha_1\right)\left(\sin\left(\theta+\beta\right)-e^{\theta\tan\phi}\sin\beta\right)}{\sin\alpha_1}\right] \quad (23)$$

Table 1 Static bearing capacity coefficient ($N_{\gamma e}$) for $k_h = 0$, $k_v = 0$

Ø	$2c/\gamma B_0$	D_f/B_0			
		0.25	0.5	0.75	1
Static condition					
20°	0	4.399	8.079	11.746	14.713
	0.25	4.644	8.331	11.992	14.962
	0.5	4.888	8.579	12.237	15.212
25°	0	6.373	12.875	18.428	23.002
	0.25	6.735	13.237	18.797	23.386
	0.5	7.096	13.599	19.167	23.767
30°	0	11.159	21.751	34.045	45.747
	0.25	11.737	22.349	34.647	46.353
	0.5	12.316	22.947	35.248	46.959

where OX and OY are the lever arm of the passive resistances P_{Pq}, P_{Pc} and $P_{P\gamma}$, respectively.

$$\overline{OX} = r_0\left[\frac{\left(e^{\theta\tan\phi}\sin\beta - \sin(\theta+\beta)\right)\cos\phi}{2\sin\alpha_1} - \cos\left(\alpha_1+\theta+\beta-\phi\right)\right]$$

$$\overline{OY} = r_0\left[\frac{\left(e^{\theta\tan\phi}\sin\beta - \sin(\theta+\beta)\right)\cos\phi}{3\sin\alpha_1} - \cos\left(\alpha_1+\theta+\beta-\phi\right)\right]$$

And X and Y are horizontal and vertical distances between the center of gravity of log-spiral zone BDE and the arbitrary center of the log-spiral (O)

where $X = \frac{\int_0^\theta \int_{\frac{x_1}{2}}^{x_2} \mathrm{d}z_2}{\int_0^\theta x_1 \cdot \mathrm{d}z_2} = \frac{I_4}{I_6}$ and $Y = \frac{\int_0^\theta x_1 \cdot z_2 \cdot dz_2}{\int_0^\theta x_1 \cdot dz_2} = \frac{I_5}{I_6}$

$$x_1 = r_0\left[e^{\theta_x\tan\phi}\cos\left(\beta+\theta-\theta_x\right) - \cos(\beta+\theta)\right]$$

The values of I_1, I_2, I_3, I_4, I_5 and I_6 are evaluated by numerical integration method (Simpson 1/3 rule) using MATLAB (2013).

Now, from Eqs. (22) and (23) we can get the values of $P_{P\gamma}$ and (P_{Pq}, P_{Pc}), respectively. So,

$$P_P = P_{P\gamma} + P_{Pq} + P_{Pc} \tag{24}$$

The values of passive resistances $P_{m\gamma}$, P_{mq} and P_{mc} at a mobilization factor m can be obtained by substituting the angle Φ by Φ_m and changing the wedge angle α_1 to α_2 and α_2 to α_1 in the Equations of $P_{P\gamma}$, P_{Pq} and P_{Pc}. So,

$$P_m = P_{m\gamma} + P_{mq} + P_{mc} \tag{25}$$

Now, putting these values of P_p and P_m in Eq. (15), we can get the value of P_L. So, the ultimate single seismic bearing capacity coefficient of shallow strip footing can be given by

$$N_\gamma = {2P_L}/{\gamma B_0} \tag{26}$$

3 Result and Discussion

After optimization of bearing capacity coefficient ($N\gamma$) w.r.t. α, β, θ and t/T for different locations of the center of the log-spiral curve by iterative technique, the optimum resistance is found out using MATLAB (2013). From the global concave curve, the minimum value is taken. This process is repeated for different values of mobilization factor m. The optimized bearing capacity coefficients are obtained for the maximum value of m as it satisfies the three equilibrium conditions. These optimized bearing capacity coefficients ($N_{\gamma e}$) are presented in Tables 1, 2, 3 and 4 for static and seismic conditions ($k_h = 0.1$, 0.15 and 0.2), respectively. Here, the values of bearing capacity coefficients are given for $\xi = 10\%$ and ω_p/ω_s ratio as 1.87. The corresponding value of α_1, β and θ for optimized bearing capacity coefficients ($N_{\gamma e}$) gives the critical focus of the log-spiral failure surface for a certain condition. Steps to calculate the ultimate bearing capacity using the suggested methodology are as follows:

Table 2 Pseudo-dynamic bearing capacity coefficient ($N_{\gamma e}$) for $k_h = 0.1$

Ø	$2c/\gamma B_0$	D_f/B_0											
		$k_v = 0$				$k_v = k_h/2$				$k_v = k_h$			
		0.25	0.5	0.75	1	0.25	0.5	0.75	1	0.25	0.5	0.75	1
20°	0	3.440	6.808	10.647	13.542	3.354	6.503	10.299	13.012	3.261	6.173	9.922	12.438
	0.25	3.664	7.126	10.872	13.769	3.587	6.863	10.533	13.249	3.503	6.579	10.165	12.865
	0.5	3.935	7.431	11.096	13.997	3.879	7.207	10.799	13.486	3.817	6.965	10.766	12.932
25°	0	4.458	11.063	16.469	20.653	4.276	10.786	15.979	19.743	4.078	10.486	15.448	18.757
	0.25	4.909	11.393	16.807	21.207	4.762	11.130	16.331	20.424	4.602	10.844	15.814	19.575
	0.5	5.238	11.724	17.144	21.556	5.104	11.473	16.681	20.786	4.958	11.202	16.176	19.952
30°	0	7.458	17.911	30.271	42.034	7.171	17.371	29.630	41.286	6.858	16.786	28.936	40.475
	0.25	8.217	18.457	30.820	42.587	7.986	17.939	30.201	41.861	7.736	17.378	29.531	41.075
	0.5	8.745	19.003	31.386	43.141	8.536	18.507	30.772	42.437	8.308	17.970	30.126	41.675

Table 3 Pseudo-dynamic bearing capacity coefficient ($N_{\gamma e}$) for $k_h = 0.15$

Ø	$2c/\gamma B_0$	D_f/B_0											
		$k_v = 0$				$k_v = k_h/2$				$k_v = k_h$			
		0.25	0.5	0.75	1	0.25	0.5	0.75	1	0.25	0.5	0.75	1
20°	0	3.020	6.252	10.167	13.029	2.870	5.773	9.629	12.224	2.701	5.234	9.025	11.319
	0.25	3.305	6.599	10.382	13.247	3.186	6.184	9.857	12.455	3.051	5.717	9.267	11.564
	0.5	3.519	6.928	10.597	13.466	3.411	6.572	10.085	12.686	3.291	6.171	9.508	11.810
25°	0	3.621	10.271	15.613	19.625	3.304	9.818	14.845	18.233	2.949	9.310	13.982	16.668
	0.25	4.110	10.587	15.936	20.254	3.847	10.154	15.187	19.051	3.552	9.666	14.345	17.699
	0.5	4.425	10.903	16.259	20.588	4.181	10.488	15.529	19.405	3.907	10.022	14.709	18.075
30°	0	5.839	16.231	28.619	40.409	5.323	15.342	27.584	39.219	4.741	14.343	26.421	37.881
	0.25	6.677	16.754	29.145	40.939	6.249	15.896	28.142	39.781	5.767	14.932	27.013	38.478
	0.5	7.183	17.277	29.672	41.470	6.784	16.451	28.699	40.342	6.336	15.520	27.605	39.074

Table 4 Pseudo-dynamic bearing capacity coefficient ($N_{\gamma e}$) for $k_h = 0.2$

Ø	$2c/\gamma B_0$	D_f/B_0											
		$k_v = 0$				$k_v = k_h/2$				$k_v = k_h$			
		0.25	0.5	0.75	1	0.25	0.5	0.75	1	0.25	0.5	0.75	1
20°	0	2.634	5.741	9.724	12.558	2.408	5.078	8.991	11.474	2.146	4.306	8.137	10.211
	0.25	2.931	6.114	9.931	12.767	2.746	5.537	9.213	11.699	2.531	4.864	8.377	10.455
	0.5	3.135	6.465	10.137	12.977	2.966	5.967	9.436	11.925	2.769	5.385	8.618	10.700
25°	0	2.849	9.541	14.824	18.680	2.379	8.897	13.765	16.796	1.831	8.146	12.531	14.601
	0.25	3.374	9.844	15.134	19.376	2.976	9.224	14.099	17.745	2.513	8.501	12.892	15.843
	0.5	3.677	10.148	15.445	19.697	3.303	9.551	14.433	18.090	2.866	8.855	13.254	16.217
30°	0	4.349	14.684	27.099	38.914	3.563	13.410	25.637	37.252	2.647	11.925	23.933	35.314
	0.25	5.260	15.187	27.605	39.423	4.594	13.951	26.181	37.800	3.819	12.511	24.522	35.908
	0.5	5.745	15.689	28.110	39.933	5.117	14.492	26.725	38.348	4.385	13.096	25.111	36.501

1. Choose the depth of the foundation (D_f) and the width of the foundation (B_0).
2. Collect soil parameters such as soil friction angle (Φ), cohesion (c), unit weight of soil (γ) and seismic parameters such as horizontal and vertical seismic accelerations (k_h and k_v).
3. Calculate depth factor (D_f/B_0) and cohesion factor ($2c/\gamma B_0$).
4. Now, using the values provided in Tables 1, 2, 3 and 4 calculate seismic bearing capacity coefficient. For intermediate portion, linear interpolation is suggested.
5. Taking the value of $N_{\gamma e}$ (as calculated above), we can evaluate the ultimate bearing capacity of shallow foundation resting on c–Φ soil.

Figure 3 shows the variations of bearing capacity coefficients ($N_{\gamma e}$) with respect to horizontal seismic acceleration (k_h) at different soil friction angles ($\Phi = 20°$, 25°, 30°) for

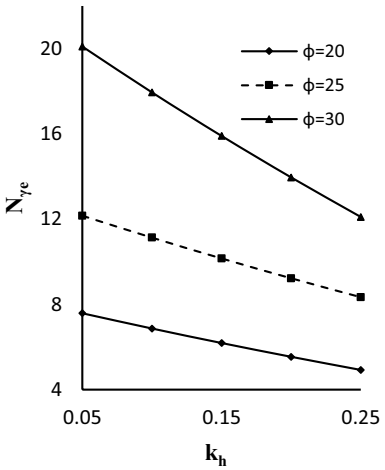

Fig. 3 Variations of bearing capacity coefficient with respect to seismic acceleration (k_h) at different soil friction angles ($\Phi = 20°$, 25°, 30°) for $2c/\gamma B_0 = 0.25$, $D_f/B_0 = 0.5$, $k_v = k_h/2$ and $m = 1$

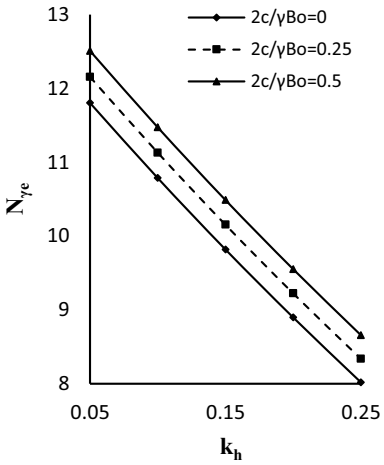

Fig. 4 Variations of bearing capacity coefficient with respect to seismic acceleration (k_h) at different cohesion factors ($2c/\gamma B_0 = 0$, 0.25, 0.5) for $\Phi = 25°$, $D_f/B_0 = 0.5$, $k_v = k_h/2$ and $m = 1$

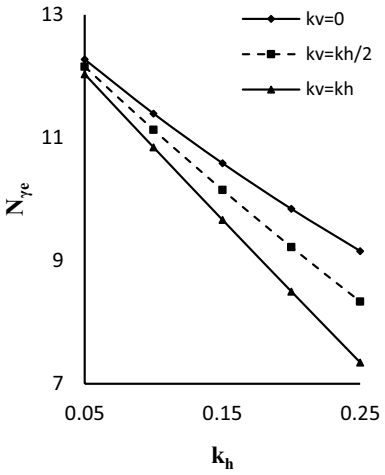

Fig. 6 Variations of bearing capacity coefficient with respect to seismic acceleration (k_h) at different vertical seismic accelerations ($k_v = 0$, $k_h/2$, k_h) for $\Phi = 25°$, $2c/\gamma B_0 = 0.25$, $D_f/B_0 = 0.5$ and $m = 1$

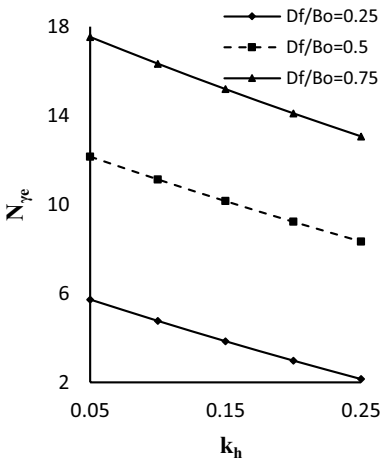

Fig. 5 Variations of bearing capacity coefficient with respect to seismic acceleration (k_h) at different depth factors ($D_f/B_0 = 0.25$, 0.5, 0.75) for $\Phi = 25°$, $2c/\gamma B_0 = 0.25$, $k_v = k_h/2$ and $m = 1$

$2c/\gamma B_0 = 0.25$, $D_f = 0.5$, $k_v = k_h/2$ and $m = 1$. It is seen that ($N_{\gamma e}$) increases with increase in soil friction angle (Φ). Due to the increase in Φ, the internal resistance of the soil particles will be increased which resembles the increase in seismic bearing capacity factors. Figure 4 shows the variations of bearing capacity coefficients ($N_{\gamma e}$) with respect to seismic acceleration (k_h) at different cohesion factors ($2c/\gamma B_0 = 0$, 0.25, 0.5) for $\Phi = 25°$, $D_f = 0.5$, $k_v = k_h/2$ and $m = 1$. It shows that ($N_{\gamma e}$) increases with an increase in cohesion factor ($2c/\gamma B_0$). Due to an increase in cohesion, seismic bearing capacity factor will be increased as an increase in cohesion causes an increase in intermolecular attraction among the soil particles which offers more bearing capacity. Figure 5 shows the variations of bearing capacity coefficients ($N_{\gamma e}$) with respect to seismic acceleration (k_h) for different depth factors ($D_f/B_0 = 0.25$, 0.5, 1) for $\Phi = 25°$, $2c/\gamma B_0 = 0.25$, $k_v = k_h/2$ and $m = 1$. It is seen that bearing capacity coefficients ($N_{\gamma e}$) increase with an increase in depth factor (D_f/B_0). Due to increase in depth factor (D_f/B_0), surcharge weight increases which increase in the passive resistance and hence increase in seismic bearing capacity factor. From Figs. 3, 4, 5 and 6, it is seen that the bearing capacity coefficients ($N_{\gamma e}$) decrease along with an increase in horizontal seismic acceleration (k_h). And Fig. 6 shows the variations of bearing capacity coefficients ($N_{\gamma e}$) with respect to seismic acceleration (k_h) at different vertical seismic accelerations ($k_v = 0$, $k_h/2$, k_h) for $\Phi = 25°$, $D_f = 0.5$, $m = 1$ and $2c/\gamma B_0 = 0.25$. It is seen that bearing capacity coefficients ($N_{\gamma e}$) decrease with the increase in vertical seismic acceleration (k_v) also. Due to an increase in seismic acceleration, the disturbances in the soil particles increase and hence decrease its resistance against bearing capacity. Figure 7 shows the variations of slip surfaces with respect to seismic acceleration ($k_h = 0.1$, 0.15, 0.2) on failure mechanism. It shows that as the seismic acceleration increases, the effect on soil media under the foundation increases. In the figure, the slip surfaces show the depth of elastic wedge increases from 1.2 to 1.7 m as k_h value increases from 0.1 to 0.2 for $B_0 = 2$ m, $\Phi = 20°$, $2c/\gamma B_0 = 0.5$, $D_f = 0.25$ and $k_v = k_h/2$.

4 Comparison of Result

On the basis of different assumptions considering different mathematical models, the bearing capacity factors are evaluated. So, each method will give its own optimized value. Table 5 shows the comparison of the pseudo-dynamic

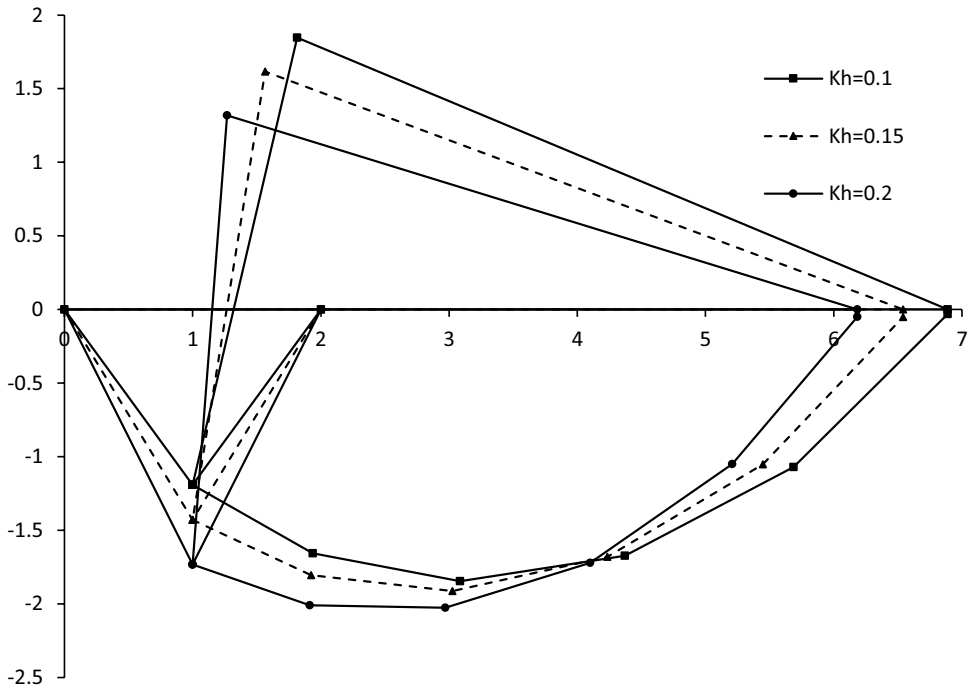

Fig. 7 Effect of slip surfaces for various values of k_h on failure mechanism

Table 5 Comparison of seismic bearing capacity coefficient ($N_{\gamma e}$) for different values of k_h and k_v with $\Phi = 30°$

Seismic analyses	$k_h = 0.1$		$k_h = 0.2$	
	$k_v = k_h/2$	$k_v = k_h$	$k_v = k_h/2$	$k_v = k_h$
Budhu and Al-Karni (1993)	10.21	9.46	3.81	2.86
Soubra (1997) (M1)	15.6 ($k_v = 0$)		8.9 ($k_v = 0$)	
Soubra (1997) (M2)	18.9 ($k_v = 0$)		10.9 ($k_v = 0$)	
Choudhury and Subba Rao (2005)	8.4	7.76	2.85	2
Ghosh (2008)	20.39	20.04	9.98	8.82
Saha and Ghosh (2014)	8.98	8.34	7.75	6.48
Saha and Ghosh (2015)	11.977	10.788	10.979	4.743
Present study	7.171	6.858	3.563	2.647

bearing capacity coefficient ($N_{\gamma e}$) obtained from the present analysis with the values obtained from previous seismic analyses for different horizontal seismic accelerations (k_h) at $\Phi = 30°$. To broaden the perspectives of different authors on their same or similar type of works considering different approaches have been compared here to the present analysis. Budhu and Al-karni (1993), Soubra (1997), and Choudhury and Subha Rao (2005) determine the seismic bearing capacity coefficient considering composite failure mechanism using pseudo-static approach, whereas Ghosh (2008) and Saha and Ghosh (2014) consider linear failure surface using pseudo-dynamic approach. On the other hand, the present analysis is performed considering the log-spiral failure mechanism in which passive zone is fully log-spiral and instead of a fixed center of log-spiral it will create its own center at optimization. The pseudo-dynamic method is used to solve this problem. It has been seen that the values of seismic bearing capacity obtained from this present approach are less than all seismic analyses which are taken here for comparison. For example, the values obtained from the present analysis are less than those of Budhu and Al-karni (1993) and Soubra (1997) because they had analyzed pseudo-static bearing capacity considering composite failure mechanism with fixed log-spiral focus. Again, the values obtained from the present analysis are much closer to those of Choudhury and Subha Rao (2005) analysis because they had also considered arbitrary log-spiral focus but pseudo-static analysis with composite failure mechanism. On the other hand, Ghosh (2008), Saha and Ghosh (2014) and Saha and Ghosh (2015) considered pseudo-dynamic analysis assuming Coulomb failure mechanism and composite failure mechanism, so the present seismic bearing capacity coefficient ($N_{\gamma e}$) is much less than from these analyses, respectively.

5 Conclusion

A mathematical model is suggested to evaluate modified pseudo-dynamic bearing capacity of shallow strip footing resting on c–Φ soil.

A fully log-spiral shear failure zone with arbitrary focus is assumed to analyze this problem using limit equilibrium method.

A single bearing capacity coefficient is proposed for the simultaneous resistance of unit weight, surcharge and cohesion.

Optimization of the seismic bearing capacity coefficient is done, and results are presented in tabular non-dimensional form.

The effects of various parameters are studied here. It is seen that the pseudo-dynamic bearing capacity coefficient ($N_{\gamma e}$) increases with increase in Φ, $2c/\gamma B_0$, D_f/B_0 and m, but it decreases with the increase in horizontal and vertical seismic acceleration (k_h, k_v).

The values obtained from the present analysis are thoroughly compared with available pseudo-static analysis as well as pseudo-dynamic analysis, and it is seen that the values obtained from the present study are in the lower side in comparison with the available analyses.

The values as provided in the present analysis can be used for the determination of bearing capacity; and for the intermediate portion, linear interpolation is suggested.

References

Bellezza I (2014) A new pseudo-dynamic approach for seismic active soil thrust. Geotech Geol Eng 32(2):561–576

Bellezza I (2015) Seismic active earth pressure on walls using a new pseudo-dynamic approach. Geotech Geol Eng 33(4):795–812

Budhu M, Al-Karni A (1993) Seismic bearing capacity of soils. Geotechnique 43(1):181–187

Choudhury D, Subba Rao KS (2005) Seismic bearing capacity of shallow strip footings. Geotech Geol Eng 23(4):403–418

Dormieux L, Pecker A (1995) Seismic bearing capacity of foundation on cohesionless soil. J Geotech Eng ASCE 121(3):300–303

Ghosh P (2008) Upper bound solutions of bearing capacity of strip footing by pseudo-dynamic approach. Acta Geotechnica 3:115–123

Ghosh P, Choudhury D (2011) Seismic bearing capacity factors for shallow strip footings by pseudo-dynamic approach. Disaster Adv 4(3):34–42

IS Code 6403:1981 Indian standard code of practice for determination of bearing capacity of shallow foundations. Bureau of Indian Standards, Manak Bhavan, New Delhi

Kolsky H (1963) Stress waves in solids. Dover Publications, New York

Kramer SL (1996) Geotechnical earthquake engineering. Prentice-Hall, Upper Saddle River

Kumar J, Ghosh P (2006) Seismic bearing capacity for embedded footings on sloping ground. Geotechnique 56(2):133–140

MATLAB (2013) The language of technical computing (Computer software), License no. 874166. The Mathworks, Inc., US

Meyerhof GG (1957) The ultimate bearing capacity of foundations on slopes. In: Proceedings of 4th international conference on soil mechanics and foundation engineering, London vol 1, pp 384–386

Meyerhof GG (1963) Some recent research on the bearing capacity of foundations. Can Geotech J 1(1):16–26

Pain A, Choudhury D, Bhattacharya SK (2015a) Seismic stability of retaining wall-soil sliding interaction using modified pseudo-dynamic method. Geotech Lett 5:56–61

Pain A, Choudhury D, Bhattacharya SK (2015b) Seismic uplift capacity of horizontal strip anchors using a modified pseudo-dynamic approach. Int J Geomech ASCE, ISSN 1532-3641

Pain A, Choudhury D, Bhattacharya SK (2016) The seismic bearing capacity factor for surface strip footings. In: Geo-Chicago 2016: sustainability and resiliency in geotechnical engineering, GSP-269. ASCE, USA, pp 197–206

Prandtl L (1921) Uber die eindringungstestigkeit plastisher baustoffe und die festigkeit von schneiden. Z Angew Math Mech 1(1):15–30 **(in German)**

Richards R, Elms DG, Budhu M (1993) Seismic bearing capacity and settlements of foundations. J Geotech Eng ASCE 119(4):662–674

Saha A, Ghosh S (2014) Pseudo-dynamic analysis for bearing capacity of foundation resting on c–Φ soil. Int J Geotech Eng 9(4):379–387

Saha A, Ghosh S (2015) Pseudo-dynamic bearing capacity of shallow strip footing resting on c–Φ soil considering composite failure surface: bearing capacity analysis using pseudo-dynamic method. Int J Geotech Earthq Eng 6(2):12–34

Saran S, Agarwal RK (1991) Bearing capacity of eccentrically obliquely loaded footing. J Soil Mech Found Div ASCE 117(11):1669–1690

Soubra AH (1993) Discussion on seismic bearing capacity and settlements of foundations. J Geotech Eng ASCE 120(9):1634–1636

Soubra AH (1997) Seismic bearing capacity of shallow strip footings in seismic conditions. Proc Inst Civil Eng Geotech Eng 125(4):230–241

Soubra AH (1999) Upper bound solutions for bearing capacity of foundations. J Geotech Geoenviron Eng ASCE. 125(1):59–69

Terzaghi K (1943) Theoretical soil mechanics. Wiley, New York

Vesic AS (1973) Analysis of ultimate loads of shallow foundations. J Soil Mech Found Div ASCE 99(1):43–45

Yuan C, Peng S, Zhang Z, Liu Z (2006) Seismic wave propagation in Kelvin–Voigt homogeneous visco-elastic media. Sci China Ser D Earth Sci 49(2):147–153